Can internal shocks produce the variability in GRBs?

Shiho Kobayashi[1], Tsvi Piran[2] and Re'em Sari[3]
Racah Institute of Physics, Hebrew University, Jerusalem 91904, Israel

Abstract

We discuss the possibility that gamma-ray bursts result from internal shocks in an ultra-relativistic matter. Using a simple model we calculate the temporal structure and we estimate the efficiency of this process. In this model the ultra-relativistic matter flow is represented by a succession of shells with random values of the Lorentz factor. We calculate the shocks that take place between those shells and we estimate the resulting emission. Internal shocks can produce the highly variable temporal structure observed in most of the bursts provided that the source emitting the relativistic flow is highly variable. The observed peaks are in almost one to one correlation to the activity of the emitting source. A large fraction of the kinetic energy is converted to radiation. The most efficient case is when an inner engine produces shells with comparable energy but very different Lorentz factors. It also gives the most preferable temporal structure.

1 introduction

The Burst and Transient Source Experiment (BATSE) on Compton-GRO has revolutionized our ideas about the location of gamma-ray bursts(GRBs). The isotropy of the events and the paucity of week bursts strongly support the cosmological origin of GRBs (Meegan et al. 1992; Paczyński 1992; Piran 1992; Nemiroff et al. 1994). The most fascinating mechanisms for producing cosmological GRBs is decelerations of ultra relativistic matter having a Lorentz factor $\gamma \geq 100$. This provides the only known solution to the compactness problem (Piran 1996). The kinetic energy of the ultra-relativistic matter is converted into internal energy by relativistic shocks. These shocks

[1]shiho@alf.fiz.huji.ac.il
[2]tsvi@shemesh.fiz.huji.ac.il
[3]sari@shemesh.fiz.huji.ac.il

can be due to the inter stellar medium (ISM), "external shocks" or inside the shell itself due to non-uniform velocity "internal shocks". Electrons are heated by the shocks and the internal energy is then radiated via synchrotron emission and inverse Compton scattering. Though the ultra relativistic matter flow was originally considered in the dynamical context of fireball(Shemi & Piran 1990; Paczyński 1990), one can imagine GRB models in which the fireball is replaced by some unknown non-thermal acceleration mechanism but the radiation still originate from slowing down of the ultra relativistic matter (Piran 1996).

Most of bursts have a highly variable temporal profile with a time scale of variability δT significantly shorter than the overall duration T. Typical value is $\delta T/T \sim 10^{-2}$. Clearly any GRB model must be able to explain this complex temporal structure.

The naive external shocks scenario requires only one uniform shell. The complex structure is due to surrounding matter (ISM in some models and star light in others (Shaviv & Dar 1995)). Two of us have shown that the efficiency of this process is less than 1% (Sari & Piran 1997a). Using the observed variability scale δT one can estimate the typical size of a single emitter. The number of emitters must be less than the number of peaks. The total area of all emitters is therefore only a $\sim 1\%$ of the shell's area. Even a modified version of this model, in which the shell is composed of many smaller shells that collide one after the other with the ISM is impossible. Most of the collisions would occur at a radius which satisfies $R \geq \Delta\gamma^2$ where Δ is the total width of the shells[4]. At this radius angular spreading (Katz 1994; Fenimore et al. 1996) will cause each peak to be spread on time scale of $R/\gamma^2 c = \Delta/c$ which is also the total duration of the bursts. The observed bursts will therefor be smooth. The only way out, in the context of the external shock model is if the shell is replaced by a narrow and highly variable beam. However, the angular width of this beam bust be than $\delta T/(T\gamma) \approx 10^{-4}$!

The obvious alternative is the internal shock scenario (Rees & Mészáros, 1994; Narayan, Paczyński & Piran, 1992). These shocks could occur within a variable relativistic wind produced by a highly variable source. Internal

[4]Distances, time, velocities β and and the corresponding Lorentz factors γ, are measured in the observer's rest frame. Thermodynamic quantities are measured in the fluid rest frame.

shocks do not suffer from the angular spreading problem. A fast shell that was injected after a slower one will eventually catch up and collide with it. If both shells have Lorentz factor of order γ, the time until collisions will be of order of $\gamma^2 L/c$, where L is the initial separation between the shells. The collision will therefor occur at radius $R = \gamma^2 L$ and the angular spreading time is of order of L/c. Since the total duration is given by the total width of the shells $\Delta/c \gg L/c$, the observed peak width is considerably smaller than the total width and complex temporal structure is possible. In view of the difficulties within the external shock scenario it is worthwhile to consider the question whether internal shocks could actually produce the temporal structure observed in GRBs and what would be the efficiency of this process.

To examine the energy conversion in internal shock we construct, following (Mochkovitch Maitia & Marques, 1995) a simple model in which the ultra-relativistic wind is represented by many shells having a random distribution of intrinsic parameters. We calculate the energy conversion due to shocks that form between the shells, considering at each time a binary (two shells) encounter. We show that internal shocks can produce the observed highly variable temporal profiles. We reproduce the result of Mochkovitch, Maitia & Marques (1995) who concluded that the efficiency of this process is low ($< 10\%$) if the spread in Lorentz factors is small. However, we show that higher efficiency could be achieved if the spread in the Lorentz factors of the ultra-relativistic matter is larger.

We explore in section 2 the basic unit of our model, the interaction of two shells. We explain in section 3 the algorithm for evolution of multiple shells. In section 4 and 5, we discuss the temporal structure and the efficiency, respectively. Finally we discuss the implication to observation in section 6.

2 Two shell interaction

Internal shocks arise in a relativistic wind with a non uniform Lorentz factor and convert a portion of the kinetic energy to a radiation. We represent the irregular wind by a succession of relativistic shells. A collision of two shells is the elementary process in our model.

A rapid shell (denoted by the subscript r) catches up a slower one (s) and the two merge to form a single one (m). The system behaves like an inelastic collision between two masses m_r and m_s. Using conservation of energy and

momentum we calculate the Lorentz factor of the merged shell to be

$$\gamma_m \simeq \sqrt{\frac{m_r\gamma_r + m_s\gamma_s}{m_r/\gamma_r + m_s/\gamma_s}}, \tag{1}$$

where $\gamma_i(\gg 1)$ and m_i are the Lorentz factors and the masses of these shells. The internal energy of the merged shell is the difference of kinetic energy before and after the collision:

$$E_{int} = m_r c^2(\gamma_r - \gamma_m) + m_s c^2(\gamma_s - \gamma_m). \tag{2}$$

The efficiency of conversion of the kinetic energy into the internal energy in a single collision is given by

$$\epsilon = 1 - (m_r + m_s)\gamma_m/(m_r\gamma_r + m_s\gamma_s). \tag{3}$$

The emitted radiation will be observed as a pulse with a width δT. Three time scales, the cooling time, the hydrodynamic time, and the angular spreading time determine δT [5]. The internal energy is radiated via synchrotron emission and inverse Compton scattering. In most of cases, the cooling time scale of electrons is much shorter than the hydrodynamic time scale (Sari et al. 1996; Sari & Piran 1997b), so we can neglect the cooling time.

The hydrodynamic time scale is the time that the shock crosses the shell. In fact there are two shocks as the interaction between the two shells takes place in the form of two shocks: a forward shock and a reverse shock. Using conservation of mass, energy and momentum at the shocks and equality of pressures and velocities along the contact discontinuity, one can derive the Lorentz factors of the forward and the reverse shocks γ_{fs}, γ_{rs} (Sari & Piran 1995):

$$\gamma_{fs} \simeq \gamma_m\sqrt{\left(1 + \frac{2\gamma_m}{\gamma_s}\right) / \left(2 + \frac{\gamma_m}{\gamma_s}\right)}, \quad \gamma_{rs} \simeq \gamma_m\sqrt{\left(1 + \frac{2\gamma_m}{\gamma_r}\right) / \left(2 + \frac{\gamma_m}{\gamma_r}\right)}. \tag{4}$$

[5]Clearly, if the source is located at a high redshift z, all the observed time scales are stretched by a factor $1 + z$. However, as we are interested mainly in the ration between the width of the peaks and the overall duration and in the efficiency energy conversion this factor is unimportant.

For simplicity, we estimate the emission time scale by the time that the reverse shock crosses the rapid shell:

$$\delta t_e = l_r/c(\beta_r - \beta_{rs}). \tag{5}$$

where l_r is a width of the rapid shell. The emitting region moves towards the observer, the observed time scale is shorter by a factor of $1/2\gamma_m^2$. If both shells have Lorentz factor of order γ, this observed time scale is of order l_r/c.

If the collision of the shells takes place at a large radius R, angular spreading effects the width of the pulse. The separation of the shells is L, the effect of angular spreading on the pulse width is $\sim L/c$ as we mentioned in section 1. If the separation L is larger than the width of the shells l, the pulse width δT is determined by angular spreading. The shape of the pulse become asymmetric with a fast rise and a slower decline (Fig. 1) which GRBs typically show. The peak amplitude is given by $E_{int}c/l$. If angular spreading is significant, the amplitude is lower by a factor of $1-(1+l/L)^{-2}$. The observed luminosity, $\mathcal{L}$ is given by

$$\mathcal{L}(t) = \begin{cases} 0, & (t<0), \\ h\left[1-1/(1+2\gamma_m^2 ct/R)^2\right], & (0<t<\delta t_e/2\gamma_m^2), \\ h\left[1/(1+(2\gamma_m^2 t-\delta t_e)c/R)^2 - 1/(1+2\gamma_m^2 ct/R)^2\right], & (t>\delta t_e/2\gamma_m^2), \end{cases} \tag{6}$$

where $h = E_{int}2\gamma_m^2/\delta t_e$.

We assume that the internal energy produced by the collision is radiated isotropically in the shell's rest frame. We also assume that all the internal energy is radiated rapidly. In this case we obtain at the end of the collision a single cold shell whose Lorentz factor is γ_m, given by Eq. 1. The shocks compress the initial shells and it results in a thinner shell with a width l_m:

$$l_m = l_s\frac{\beta_{fs}-\beta_m}{\beta_{fs}-\beta_s} + l_r\frac{\beta_m-\beta_{rs}}{\beta_r-\beta_{rs}}. \tag{7}$$

The density is discontinuous through the contact discontinuity. For simplicity we average the density:

$$\rho_m = \frac{\rho_r l_r\gamma_r + \rho_s l_s\gamma_s}{l_m\gamma_m}. \tag{8}$$

We describe the resulting shell as a homogeneous shell with a constant density ρ_m and a Lorentz factor γ_m.

While the shells propagate, their density decrease due to the spherical geometry. However the density ratio between any two shells remain constant and the process depends just on the density ratio and not on the absolute value of the density. We expect therefor that this one dimensional model captures the basic features of realistic events.

3 The Multiple shell model

We represent the irregular wind by a succession of relativistic shells with a random distribution of Lorentz factors and densities. A collision between two shells produce shocks which convert some of the kinetic energy of the shells to thermal energy. The thermal energy is then radiated via synchrotron emission and inverse Compton scattering. In section 2, we calculated the observed radiation produced by a collision between two shells. For multiple shells, numerous collisions take place. Each collision produces a pulse similar to that shown in Fig. 1. To construct the temporal structure in a given model we calculate the time sequence of the two shell collisions and we superimpose the resulting pulses from each collision.

Consider a wind consisting of N shells. We assign an index i, $(i = 1, N)$ to each shell according to the order of the emission from the inner engine. Each shell is characterized by four variables: a Lorentz factor γ_i, a density ρ_i, (the shells are cold and therefore the pressure satisfies $p_i \equiv 0$.) a width l_i and the time, $\tilde{t}_i$, when the shell was ejected from the source. We choose the origin of time such that the last shell - the N-th shell - is emitted at $\tilde{t}_N = 0$. Clearly all other shells are emitted earlier so the $\tilde{t}_i$'s are negative for $i < N$. At $t = 0$ the shells are at the following "initial" positions (inner edge): $R_i = -\tilde{t}_i \beta_i c$. We denote the distance at this stage between the shell i and the shell $i + 1$ by L_i: $L_i \equiv R_i - R_{i+1} - l_{i+1}$. The time l_i/c corresponds to the period that the "inner engine" has operated, while L_i/c corresponds to the period for which the "inner engine" was quiet. The size of the inner engine should be, of course, smaller than l to produce a shell with a width l.

We turn now to evaluate the evolution of this multiple shell system. There will be numerous collisions between different shells. We denote by the index j the j-th collision which takes place at a time t_j and position $R_c(t_j)$. For simplicity we define a zeroth collision at the initial time $t_0 = 0$ this enables us to put the first collision on par with the rest. Given the velocities of the

shells β_i and their separation L_i at t_{j-1} we calculate for all pairs $(i, i+1)$ satisfying $\beta_{i+1} > \beta_i$ the collision time:

$$\delta t_{i,i+1} \equiv L_i/c(\beta_{i+1} - \beta_i). \tag{9}$$

We then find the minimal collision time among all the δt_i's:

$$\delta t_j = \min[\delta t_{i,i+1}]. \tag{10}$$

Let s and $s+1$ be the index of the shells for which this minimum takes place. The j-th collision is between the s and $s+1$ shells and takes place at the time

$$t_j = t_{j-1} + \delta t_j \tag{11}$$

and at the position

$$R_c(t_j) = R_{s+1}(t_j) = R_{s+1}(t_{j-1}) + c\beta_{s+1}\delta t_j. \tag{12}$$

An observer at R_0 away from the central source will begin to detect radiation from this collision at a time

$$t_{obs,s} = (R_0 - R_c(t_j))/c + t_j. \tag{13}$$

Note that, for reasons that will be clear later we give this observed time the index s of the outer shell that participated in the collision. At the end of the computation we set the minimum of $t_{obs,s}$ to be the origin of the observer time as this is when the first radiation is observed. We assign the pulse shape presented in section 2 beginning at this time to the overall observed signal.

We rearrange the shells after each collision as follows. Each shell moves from its earlier position $R_i(t_{j-1})$ to

$$R_i(t_j) \equiv R_i(t_{j-1}) + c\beta_i\delta t_j \tag{14}$$

For the first collision $t_{j-1} = 0$ and we use the "initial positions" here. All the shells except the s shell and the $s+1$ shell keep their Lorentz factor, the density and the width: γ_i, ρ_i and l_i. The s and the $s+1$ shell merge to form a single shell which we label $s+1$. We delete the s shell and we will skip from now on this index when it will be encountered. Using the results of section 2 we calculate now the new parameters for the $s+1$ shell: γ_{s+1}, ρ_{s+1} and l_{s+1}.

We return now to the calculation of the distances between shells: L_i and the corresponding collision time δt_i. We find the next collision and proceed until there are no more collisions, i.e., until all the shells have merged to form a single shell or until the shells are ordered with increasing values of the Lorentz factor.

In order to reduce the number of parameters describing the wind we adopt the following simplifications. We assume a constant initial width $l_i = l$ and constant initial separation $L_i = L$. In other words, we assume that the "inner engine" operates for a fixed period l/c and then it is quiet for a fixed period L/c.

We assume that the Lorentz factor of each shell is uniformly distributed between γ_{min} and γ_{max}. For the distribution of the density we have two kinds of models. In the first kind we consider models in which the density, the mass or the energy of each shell is a random variable which is uniformly distributed between 1 and some maximal value X_{max}. In the second kind the density is correlated with the Lorentz factor as $\rho_i \propto \gamma_i^{\eta-1}$ so that the mass and kinetic energy of each shell are proportional to γ_i^{η} and $\gamma_i^{\eta+1}$ respectively.. For $\eta = 1$ the shells have equal density, for $\eta = 0$ the shells have equal mass and for $\eta = -1$ the shells have equal energy. We will see later that the random density/mass/energy models give almost same efficiency as the corresponding constant model, and the dependence on X_{max} is low. We therefore present most of the result for the correlation models which are more simple.

Any time scale in this system is proportional to a sum of L and l, the amplitudes of observed peaks depends neither on the absolute value of l nor that of L. If both of L and l are transformed by the same factor, we will get similar temporal profile. We are interested in neither the absolute value of the duration nor that of the peak, then we can use a single parameter L/l instead of the two parameters L and l. The efficiency of the energy conversion by the shocks is independent of L/l. The total energy emitted is the sum of the energy emitted in the elementary two shell collisions which are independent of L/l. The density ρ is the only quantity in this system with dimensions of mass. Therefore only density ratio rather than density can determine the time scale, and the overall normalization of the density ρ is also unimportant. Consequently we find that there are only five initial parameters: N, L/l, γ_{max}, γ_{min} and either η (if the density is correlated with the Lorentz factor) or X_{max} (for random distribution of ρ,m or E).

4 Temporal Structure

The calculated temporal structure is a superposition of the pulses from the elementary two shell collisions. Several typical temporal profiles are presented in Figs. 2a-2f. Fig. 2a depicts the luminosity for a model with $N = 100$ and $L/l = 5$ as a function of the observed time for shells with a constant energy ($\eta = -1$). During the evolution of the N shells, almost N collisions happen and almost N pulses are produced. Though some of the peaks are not observed because of their higher neighbors. The number of peaks is given by $\sim N$. In Fig. 2b the luminosity is plotted with the same parameters as Fig. 2a except that $N = 20$. Fig 2a and 2b show that N practically determines the number of peaks. The width of a given peak δT is determined by the emission time scale $\sim l/c$ or by the angular spreading $\sim L/c$. If the value of the separation L is larger than that of the width l, $\delta T/T$ is $\sim 1/N$ and independent of L/l. In Fig. 2c, the luminosity is plotted with the same parameters as Fig. 2b except that $L/l = 1$. The profile is almost independent of L/l.

The different amplitude of the peaks originate mainly from the difference in E_{int}, since all peaks have width of the same order of magnitude $\sim L/c$. For given random Lorentz factors, E_{int} depends on the index η for models with density correlated to the Lorentz factor. The random Lorentz factors are uniformly distributed between γ_{min} and γ_{max}. If $\gamma_{max}/\gamma_{min} \gg 1$, the ratio γ_r/γ_s is typically large. In such a case, we obtain a simple formula,

$$E_{int} \sim \begin{cases} (1 - 1/\sqrt{2})\gamma_r^2, & (\eta = 1), \\ 2 - \sqrt{2}, & (\eta = -1). \end{cases} \tag{15}$$

For $\eta = -1$, E_{int} takes almost the same value for most of the collisions so most of the peaks have comparable amplitude (see Fig. 2a). Thus, for $\eta = -1$ we practically observe the "shell structure" produced by the inner source as almost all two shell collisions produce an observable peak. If on the other hand $\eta = 1$ (see Fig. 2d) a few collisions produce significantly higher peaks than others and only those are observed. Thus the number of the observed peaks is much less than N, the observed temporal structure corresponds only weakly to the activity of the inner source. Visual inspection suggests that the temporal structure produced by $\eta = -1$ resembles better the observed temporal structure.

Fig. 2e and Fig. 2f present the luminosity profiles for model with random energy and random density respectively.. Both use $X_{max} = 1000$ and both with spread of Lorentz factor $\gamma_{max}/\gamma_{min} = 10$. Again the random density is more spiky than the random energy case. However as could be guessed intuitively, the random energy and the random density cases are more spiky than the constant energy ($\eta = -1$, Fig. 2a) and constant density ($\eta = 1$, Fig. 2d) respectively..

The total width of the wind is $\Delta = Nl + (N-1)L$. Neighboring shells collide on a time scale of $L\gamma^2/c$, with fluctuations of the same order of magnitude due to the fluctuations of γ. The matter is moving toward the observer, the resulting observed time scale is L/c. On the other hand, the difference in observed time due to the location of the given shell within the wind is a order of Δ/c. Since by definition $\Delta \gg L$ we observe pulses arising from collision between shells mostly according to their positions inside the wind, i.e., according to the time that those shells were emitted by the inner engine. In Fig. 3, we plot the time that radiation is observed from a shell $t_{obs,s}$ versus the time that the shell was ejected from the source $\tilde{t}_s$. We associated the emission from a given collision with the slower shell. The clear correlation between the observed time and the time that the source ejected the specific shell shows that the observed temporal structure reflects the activity of the source. This conclusion is valid even if there is a large spread in γ.

5 Efficiency

We have shown that internal shocks could produce the highly variable temporal structure. We ask now what is the efficiency of this process? The relativistic shells collide with each other and merge into more massive shells. The overall efficiency of conversion of kinetic energy in internal shocks can be calculated from the initial and final kinetic energies as:

$$\epsilon = 1 - \frac{\Sigma m_i^{(f)} \gamma_i^{(f)}}{\Sigma m_i^{(i)} \gamma_i^{(i)}} \tag{16}$$

where the superscript (f) and (i) represent the initial and final values, respectively.

This efficiency depends on the parameters of the model N, γ_{min}, γ_{max} and η (or X_{max}) and on the specific realization: the set of random Lorentz

factors that are assigned to each shell. For each choice of the parameters of the model, we have evaluates the efficiency for 100 realizations. The mean efficiency and its standard deviation are listed in Table 1.

The efficiency is only a few percents if the spread in the Lorentz factor is relatively low (a factor of 2-3). This agrees with results of Mochkovitch, Maitia and Marques (1995) who concluded that the efficiency of this process is less than 10%. However, higher efficiency could be reached if the spread in γ is larger. The spread required, for example, for 10% is $\gamma_{max}/\gamma_{min} \sim 6$ for $N = 100$ and $\eta = -1$.

The efficiency is independent of L/l, which is important only for the temporal structure. For models with density correlated with the Lorentz factor the relevant parameters that determine the efficiency are N, η, γ_{min} and γ_{max} (see Table 1a). For the random density models, we evaluated the efficiency with $X_{max} = 1$ to 1000. The efficiency is almost independent of X_{max}. It can be seen that the efficiencies of the models with random n, m and E are very similar to those with $\eta = 1, 0$ and -1, respectively (Table 1b).

As the number of shells, N, increases, the kinetic energy of relative motion of the final mergers becomes negligible. The efficiency approaches an asymptotic value. Further if we consider large values of γ_{min}, the efficiency depends only on the ratio $\gamma_{max}/\gamma_{min}$ reaching an asymptotic value for large $\gamma_{max}/\gamma_{min}$ (Fig. 4). For models with correlation between the density and the Lorentz factor, this asymptotic value depends only on the index η. In the limits $\eta \to \pm\infty$, a single shell carries all the energy of the system and the energy and momenta of the other shells are negligible. Therefore, the massive shell is unaffected by collisions with the lighter ones. We expect a low efficiency in this limit (Fig. 5).

In order to understand the dependence of the efficiency on η we consider a simplified model. Let all the shell collide and merge into a single shell and only then emit the thermal energy as the radiation. Using conservation of energy and momentum we can calculate the Lorentz factor and the efficiency:

$$\gamma = \sqrt{\Sigma\gamma_i^{\eta+1}/\Sigma\gamma_i^{\eta-1}}, \tag{17}$$

$$\epsilon = 1 - \Sigma\gamma_i^{\eta}/\sqrt{\Sigma\gamma_i^{\eta-1}\Sigma\gamma_i^{\eta+1}}. \tag{18}$$

Averaging over the random variables γ_i, and assuming a large number of

shells $N \to \infty$ we obtain:

$$\langle \epsilon \rangle \sim 1 - \frac{(\gamma_{max}/\gamma_{min})^{\eta+1} - 1}{\eta + 1} \sqrt{\frac{\eta(\eta+2)}{((\gamma_{max}/\gamma_{min})^{\eta} - 1)((\gamma_{max}/\gamma_{min})^{\eta+2} - 1)}}. \quad (19)$$

This formula explains qualitatively the behavior of our numerical results. A comparison between the simulations in which the radiations is emitted right after each collision and the simplified single merge model is presented in Fig. 5b.

An interesting point to notice is that for many shell collision (both in the numerical simulation and the simple model Eq. 19) the most efficient case is where the shells have the same energy while for the two shell collision (Eq. 3) the highest efficiency is for shells with equal mass rather than equal energy.

6 Conclusions

Using a simple model, we have shown that internal shocks can produce the highly variable profile observed in most GRBs. There is a strong correlation between the time at which we observe a pulse and the emission time of the corresponding shell from the inner engine. This correlation persists even when there is a large spread in the Lorentz factor. Thus the observed temporal structure reproduces the activity of the source.

We have shown that the number of peaks is almost the same as the number of shells that the inner engine emitted. The separation between the peaks corresponds to the duration for which the inner engine was quiet. The variability of peaks height can tell as wether all shells have comparable energy (low variability in observed peak heights) or not. A systematic statistical study comparing the temporal structure produced by internal shocks with observations will be carried out in a subsequent paper.

The efficiency of this process is low (less than 2%) if the initial spread in γ is only a factor of two. However the efficiency could be much higher. The most efficient case is when the inner engine produces shells with comparable energy but with very different Lorentz factors. In this case ($\eta = -1$, and spread of Lorentz factor $\gamma_{max}/\gamma_{min} > 10^3$) the efficiency is as high as 40%. For a moderate spread of Lorentz factor $\gamma_{max}/\gamma_{min} = 10$, with $\eta = -1$, the efficiency if 20%.

We thank J.I.Katz for many useful discussion. S.K. gratefully acknowledges the support by the Golda Meir Postdoc fellowship. This work was supported in part by a US-Israel BSF grant and by a NASA grant.

Fenimore,E.E., Madras, C.D., & Nayakshin, S., 1996, *Ap.J.*, **473**, 998.
Katz, J.I. 1994, *Ap. J.*, **432**, L107.
Meegan, C.A. et al. 1992, *Nature*, **355**, 143.
Mochkovitch, R., Maitia, V., & Marques, R. 1995, in Towards the Source of Gamma-Ray Bursts, Proceeding of 29th ESLAB Symposium, eds. Bennett, K. & Winkler, C., 531.
Nemiroff, R.J., Noriss, J.P., Kouveliotou, C., Fishman, G.J., Meegan, C.A., & Paciesas, W.S. 1994, *Ap. J.*, **423**, 432.
Narayan, R., Paczyński, B., & Piran, T. 1992, *Ap. J.*, **395**, L83.
Paczyński, B. 1990, *Ap. J.*, 363, 218.
Paczyński, B. 1992, *Nature*, **355**, 521.
Piran, T. 1992, *Ap. J.*, **389**, L45.
Piran, T. 1996, in Some unsolved problems in Astrophysics, eds. Bahcall. J. & Ostriker J.P., (Princeton University Press).
Rees, M. J., & Mészaros, P. 1994, *Ap. J.*, **430**, L93.
Sari, R. & Piran,T. 1995, *Ap.J.*, **455**, L143.
Sari,R., Narayan,R. & Piran, T. 1996, *Ap.J.* , **473**, 204.
Sari, R., & Piran, T. 1997a, *Ap.J.* in press.
Sari, R., & Piran, T. 1997b, *MNRAS* in press.
Shemi, A., & Piran, T. 1990, *Ap.J.*, 365, L55.
Shaviv, N., & Dar, A. 1995, *MNRAS*, **277**, 287.

Table.1 a

N	η	γ_{min}	γ_{max}	efficiency [%]
100	1	20	1000	10.9 ± 1.4
100	1	50	1000	10.0 ± 1.3
100	1	100	1000	8.5 ± 1.1
100	1	200	1000	6.1 ± 0.7
100	1	500	1000	1.7 ± 0.2
100	0	20	1000	19.2 ± 2.9
100	0	50	1000	16.0 ± 2.3
100	0	100	1000	12.4 ± 1.6
100	0	200	1000	7.7 ± 0.9
100	0	500	1000	1.8 ± 0.2
100	-1	20	1000	25.0 ± 3.5
100	-1	50	1000	19.5 ± 2.4
100	-1	100	1000	14.1 ± 1.6
100	-1	200	1000	8.2 ± 0.9
100	-1	500	1000	1.8 ± 0.2
20	1	100	1000	7.6 ± 2.5
20	-1	100	1000	11.0 ± 3.3
1000	1	100	1000	8.7 ± 0.3
1000	-1	100	1000	15.1 ± 0.5
1000	-1	10	10000	39.3 ± 2.6

Table.1 b

N		γ_{min}	γ_{max}	X_{max}	efficiency [%]
100	random n	100	1000	1000	8.2 ± 1.2
100	random m	100	1000	1000	12.2 ± 1.6
100	random E	100	1000	1000	14.2 ± 1.6

Mean efficiency and standard deviation of the efficiency for 100 realizations of different models.

Figure captions

Fig. 1 A peak produced by a collision between two shell. The luminosity plotted versus the observer's time. The solid line corresponds to $R = c\delta t_e$ and the dotted line corresponds to $R = 0$.

Fig. 2 The observed temporal structures. The luminosity versus the observer's time, for different models
a: $\gamma_{min} = 100$, $\gamma_{max} = 1000$, $N = 100$, $\eta = -1$ and $L/l = 5$
b: $\gamma_{min} = 100$, $\gamma_{max} = 1000$, $N = 20$, $\eta = -1$ and $L/l = 5$
c: $\gamma_{min} = 100$, $\gamma_{max} = 1000$, $N = 20$, $\eta = -1$ and $L/l = 1$
d: $\gamma_{min} = 100$, $\gamma_{max} = 1000$, $N = 100$, $\eta = 1$ and $L/l = 5$
e: $\gamma_{min} = 100$, $\gamma_{max} = 1000$, $N = 100$,
random energy with $E_{max} = 1000$ and $L/l = 5$
f: $\gamma_{min} = 100$, $\gamma_{max} = 1000$, $N = 100$,
random density with $\rho_{max} = 1000$ and $L/l = 5$

Fig. 3 The time of ejection of a shell by the inner engine, $\tilde{t}_j$ versus the observed time of the photon produced in that shell, $t_{obs,j}$, for $N = 100$, $\gamma_{min} = 10$, $\gamma_{max} = 1000$, $\eta = -1$ and $L/l = 5$. The initial position 0 and 100 correspond to the inner and outer edge of the wind.

Fig. 4 The efficiency versus $\gamma_{max}/\gamma_{min}$ with 1σ error bars of 100 random simulations, for $\gamma_{min} = 10$, $N = 500$ and $\eta = -1$.

Fig. 5 The efficiency plotted versus the index η, for $\gamma_{min} = 100$, $N = 100$. The solid line corresponds to $\gamma_{max}/\gamma_{min} = 1000$, the dotted line corresponds to $\gamma_{max}/\gamma_{min} = 100$ and the dashed line corresponds to $\gamma_{max}/\gamma_{min} = 10$. a: Numerical simulation, b: Approximation by analytic formula (19)

Fig. 1

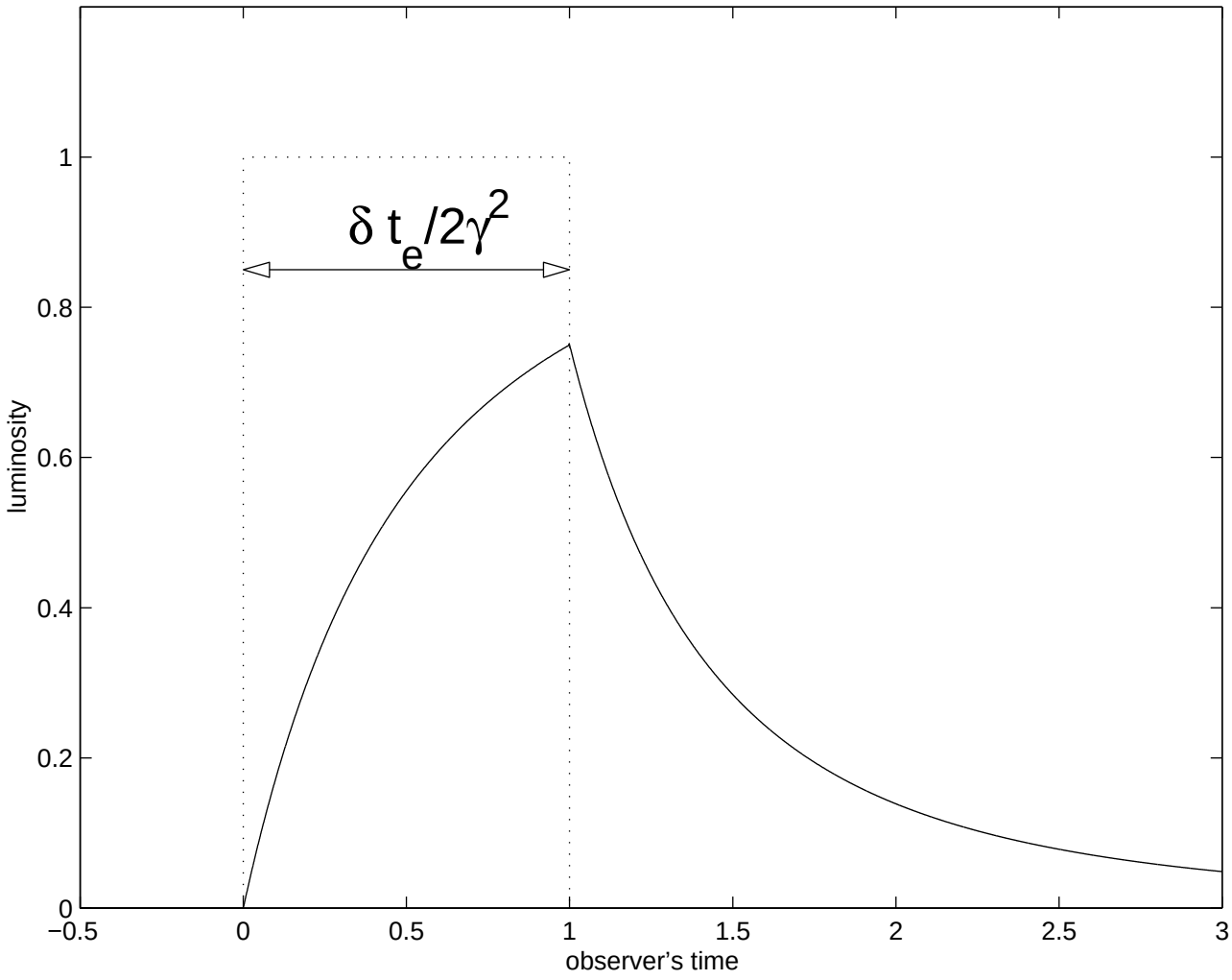
$\delta t_e/2\gamma^2$
luminosity
observer's time
0
0.2
0.4
0.6
0.8
1
−0.5
0
0.5
1
1.5
2
2.5
3

Fig. 2a

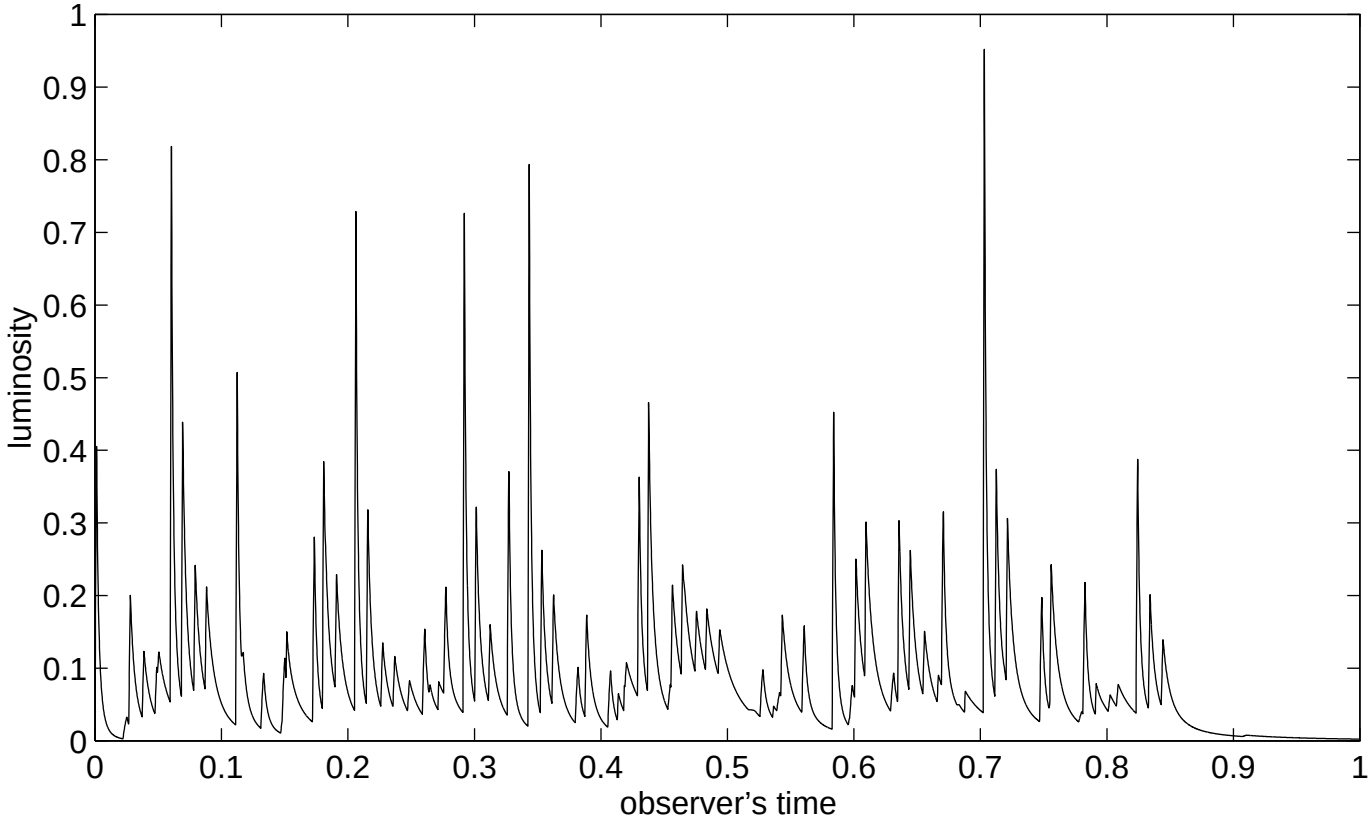
luminosity
observer's time
0
0.1
0.2
0.3
0.4
0.5
0.6
0.7
0.8
0.9
1

Fig. 2b

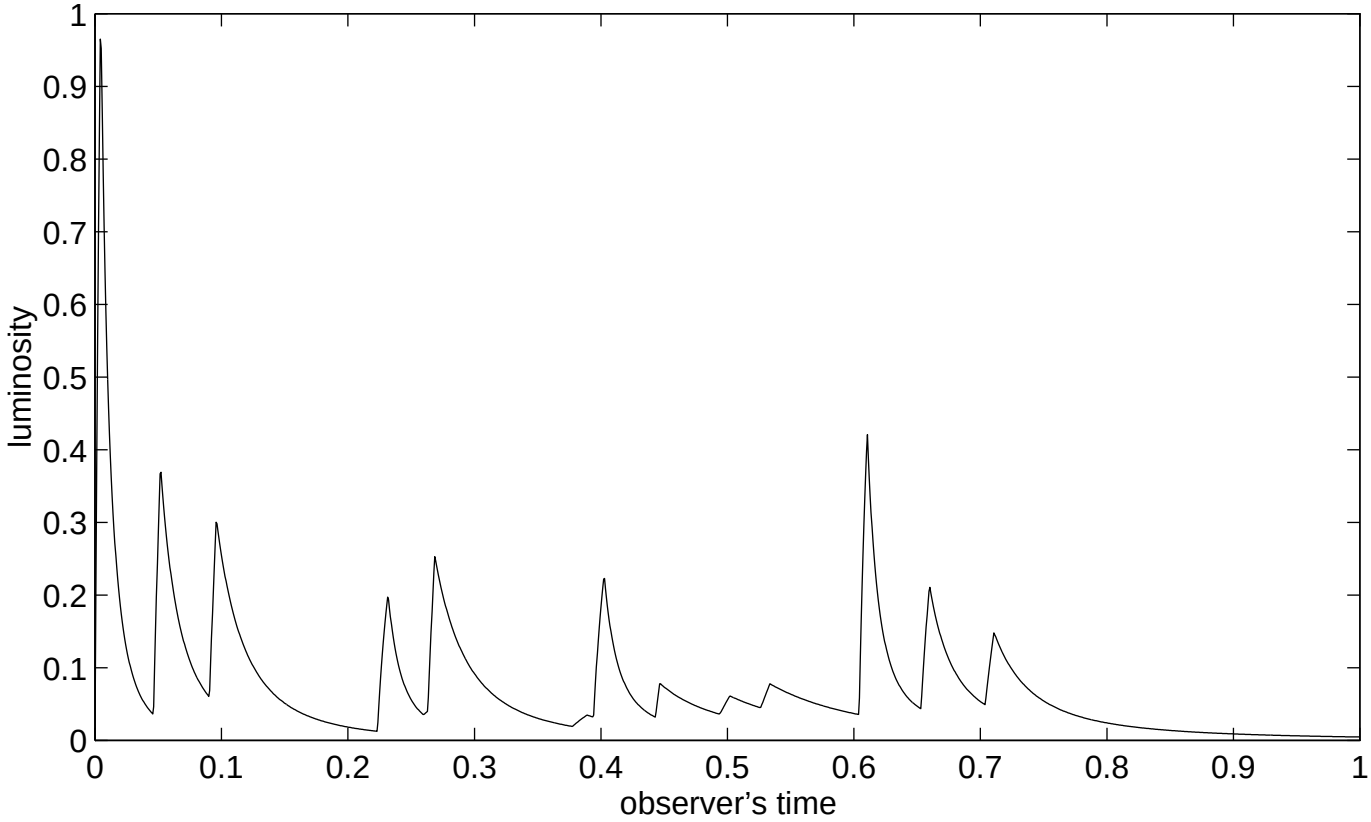
luminosity
observer's time
0
0.1
0.2
0.3
0.4
0.5
0.6
0.7
0.8
0.9
1

Fig. 2c

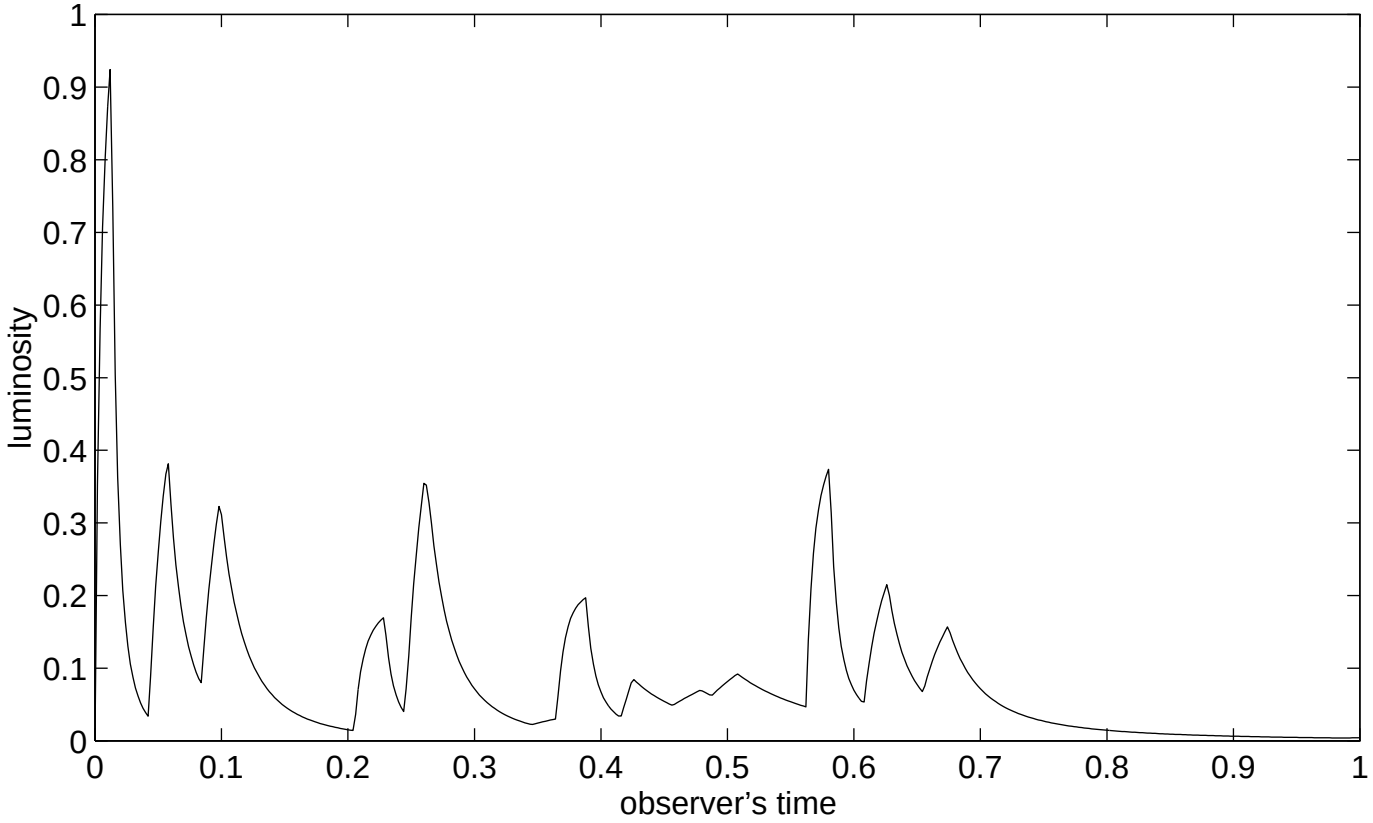
luminosity
observer's time
0
0.1
0.2
0.3
0.4
0.5
0.6
0.7
0.8
0.9
1

Fig. 2d

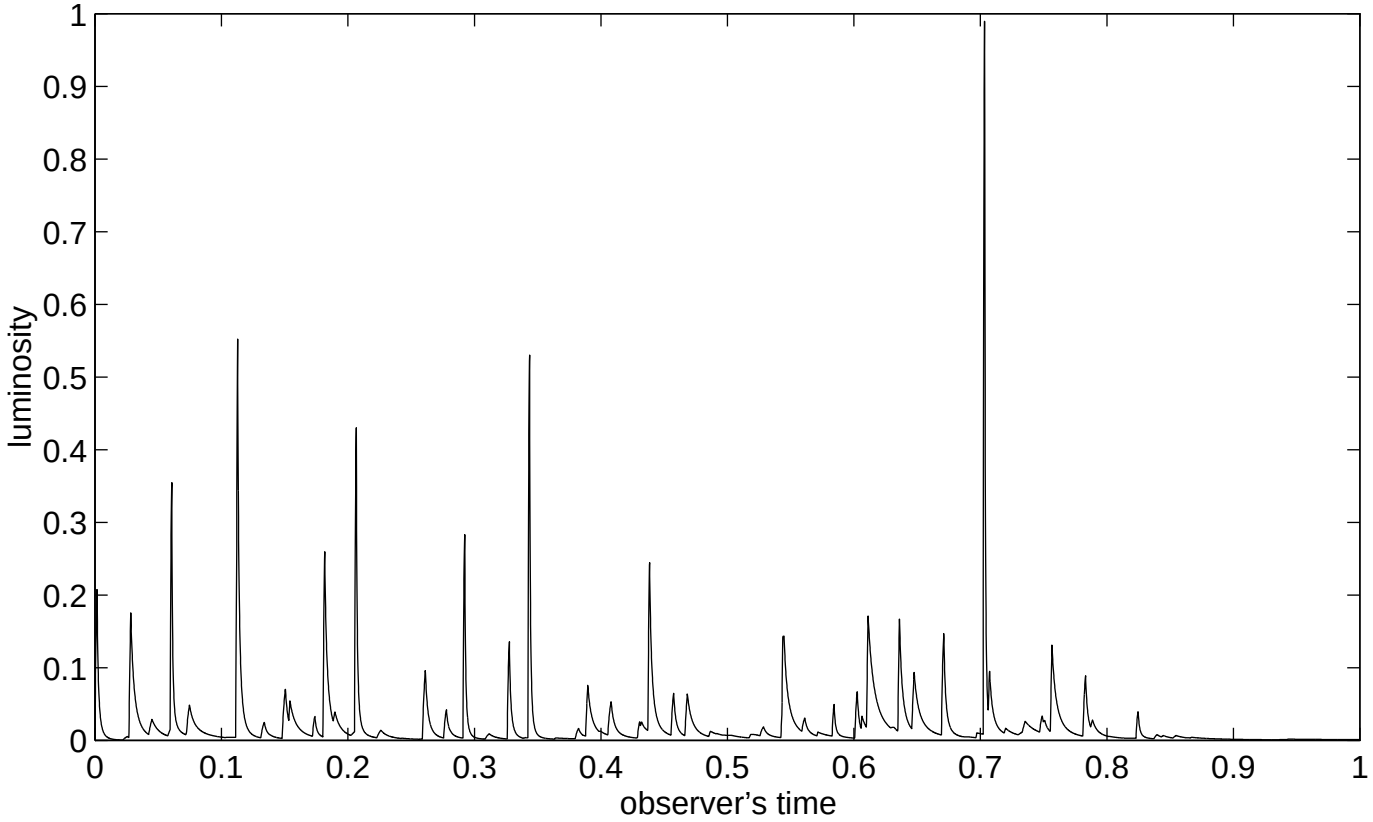
luminosity
observer's time
0
0.1
0.2
0.3
0.4
0.5
0.6
0.7
0.8
0.9
1

Fig. 2e

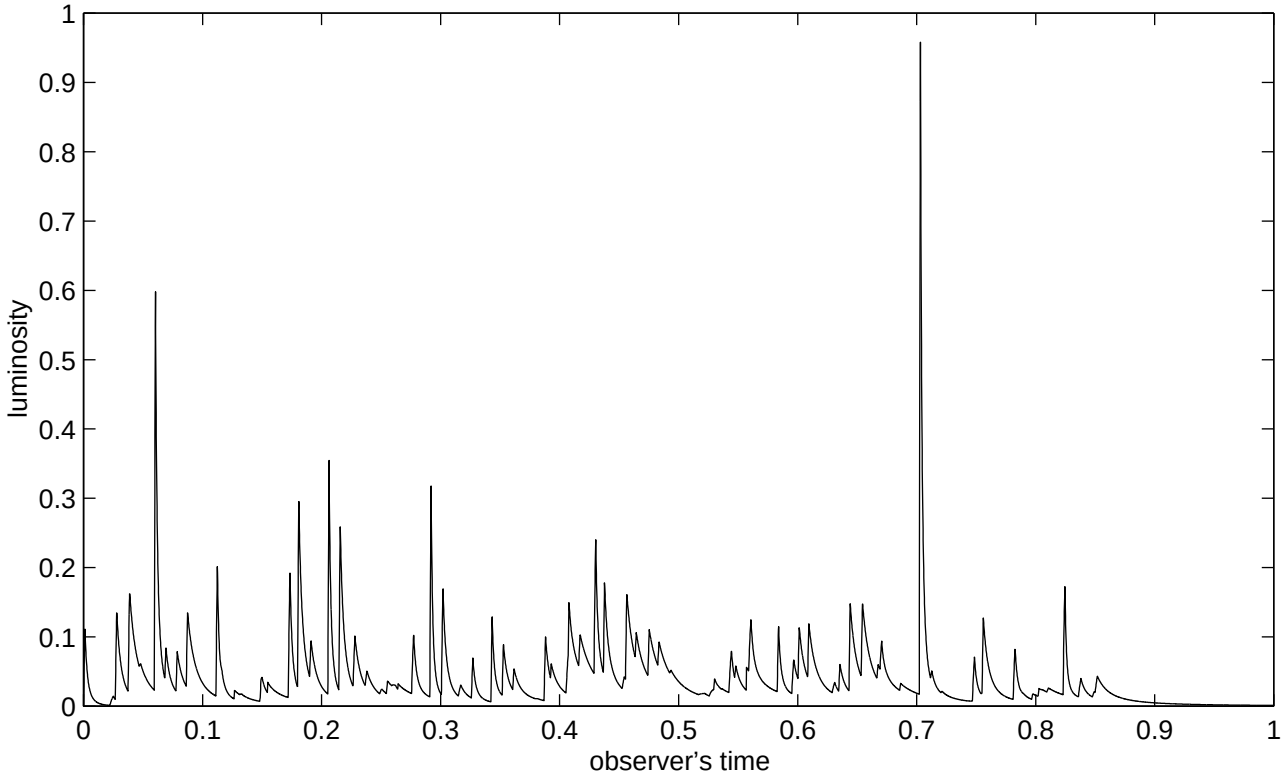
luminosity
observer's time
0
0.1
0.2
0.3
0.4
0.5
0.6
0.7
0.8
0.9
1

Fig. 2f

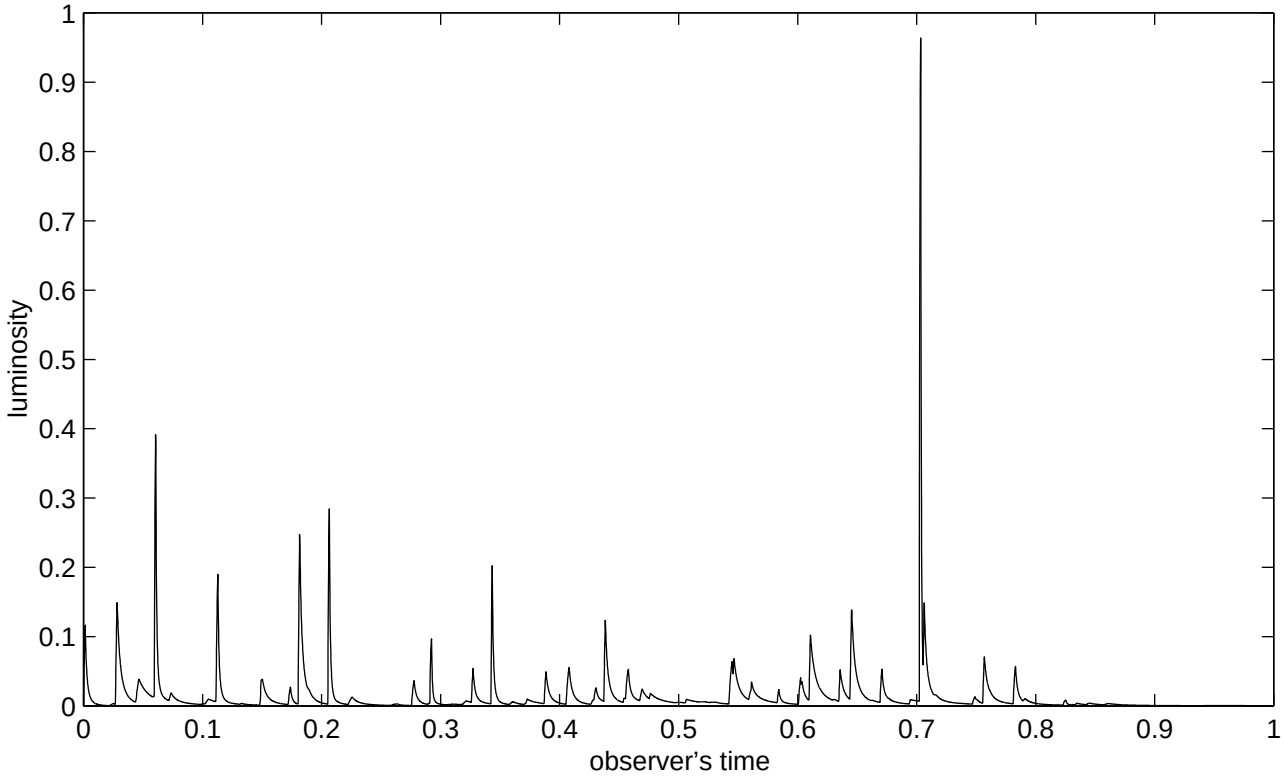
luminosity
observer's time
0
0.1
0.2
0.3
0.4
0.5
0.6
0.7
0.8
0.9
1

Fig. 3

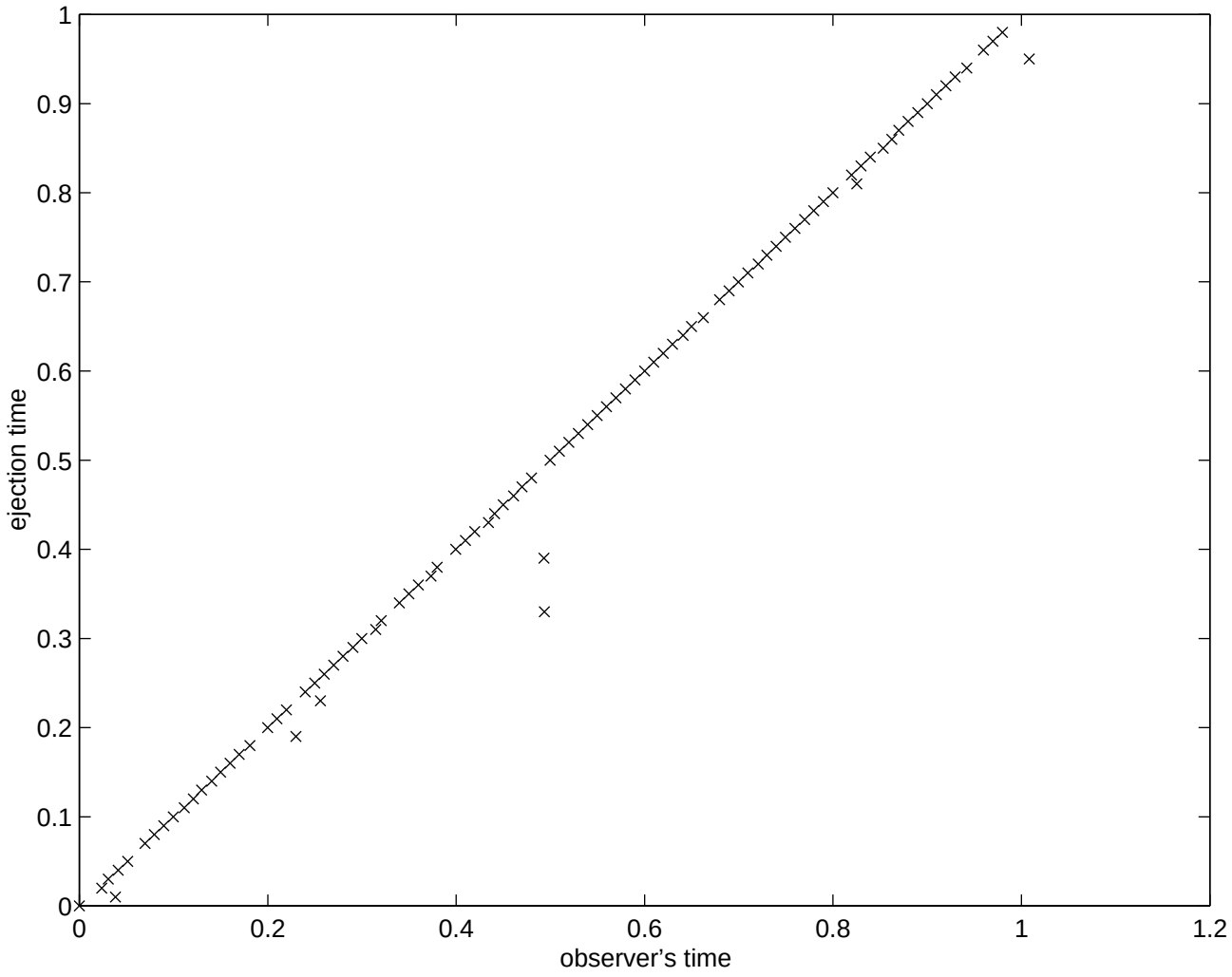
ejection time
observer's time
0
0.1
0.2
0.3
0.4
0.5
0.6
0.7
0.8
0.9
1
0
0.2
0.4
0.6
0.8
1
1.2

Fig. 4

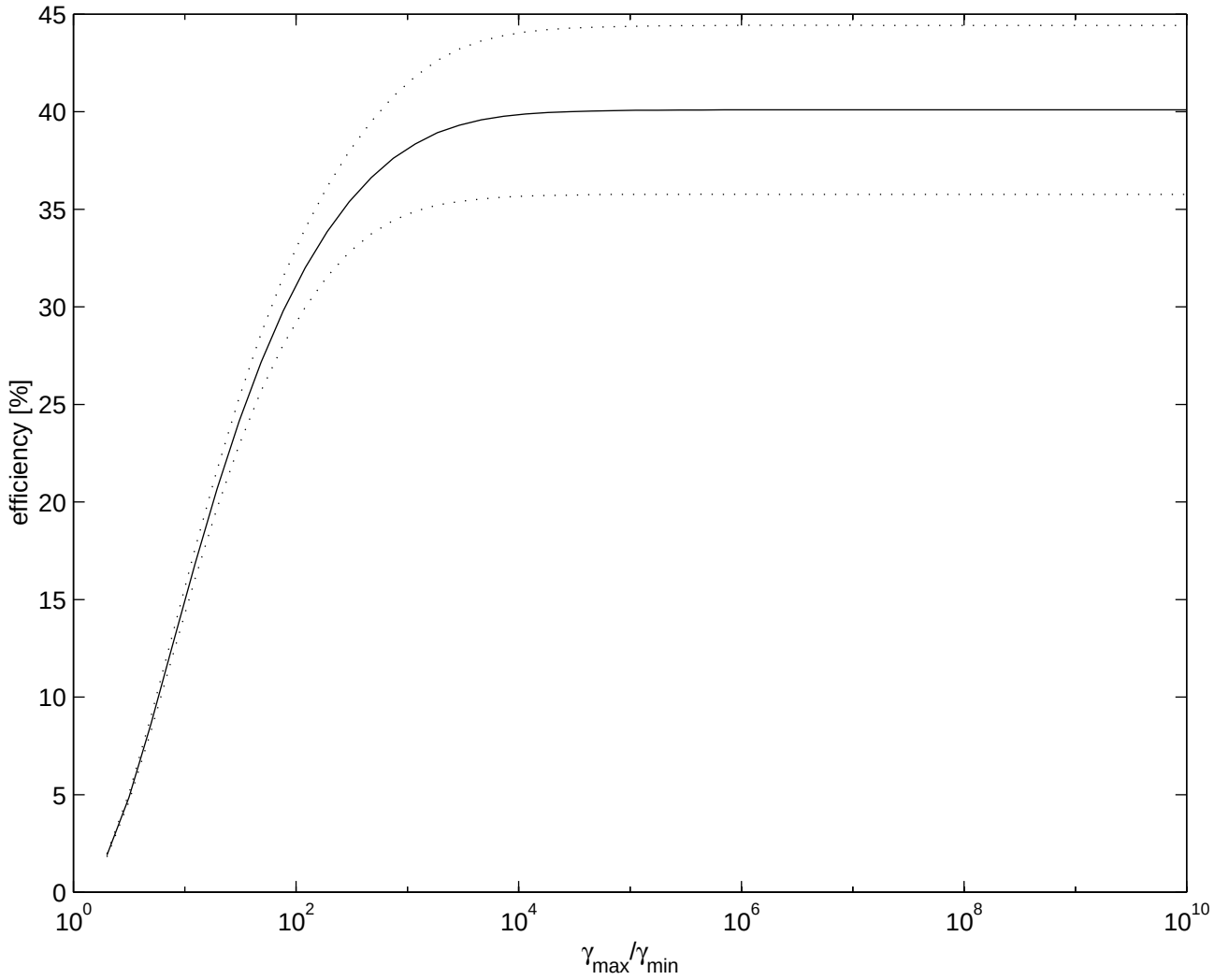
45
40
35
30
25
20
15
10
5
0
efficiency [%]
10^0
10^2
10^4
10^6
10^8
10^{10}
$\gamma_{max}/\gamma_{min}$

Fig. 5a

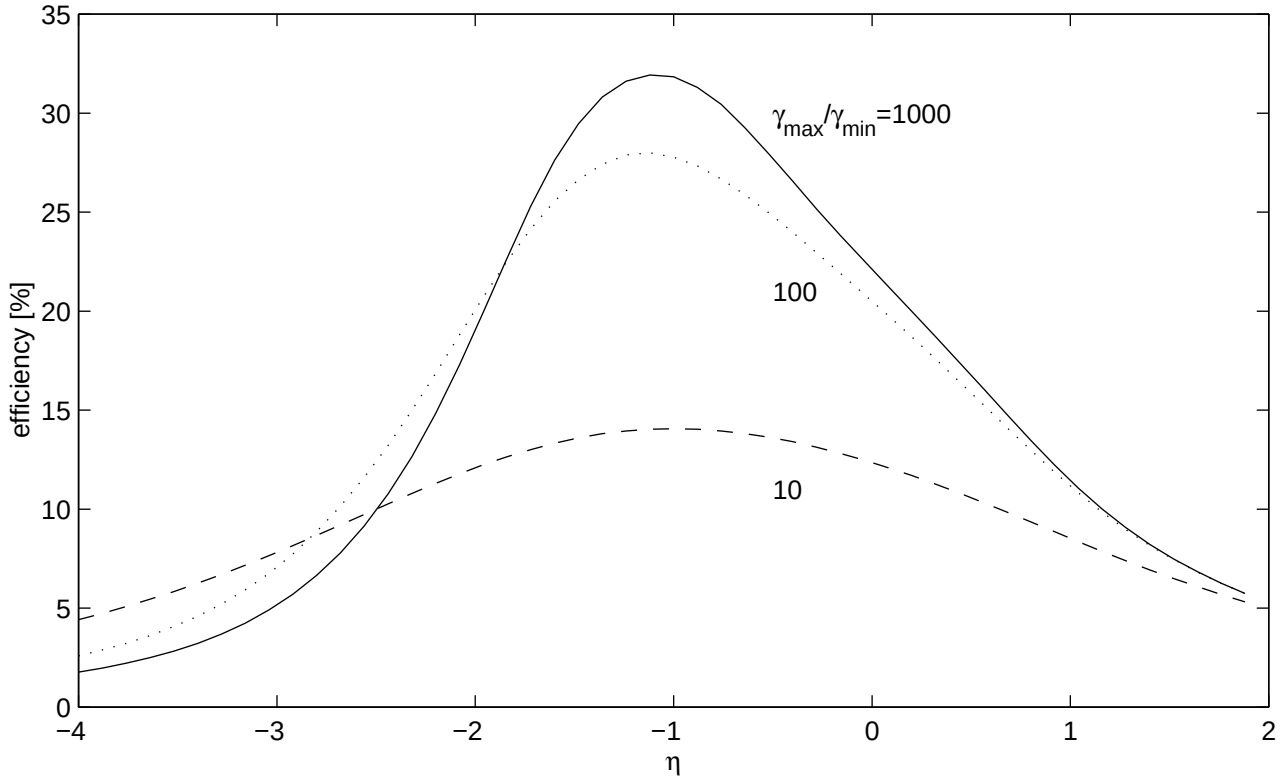
efficiency [%]
η
γmax/γmin=1000
100
10
0
5
10
15
20
25
30
35
−4
−3
−2
−1
0
1
2

Fig. 5b

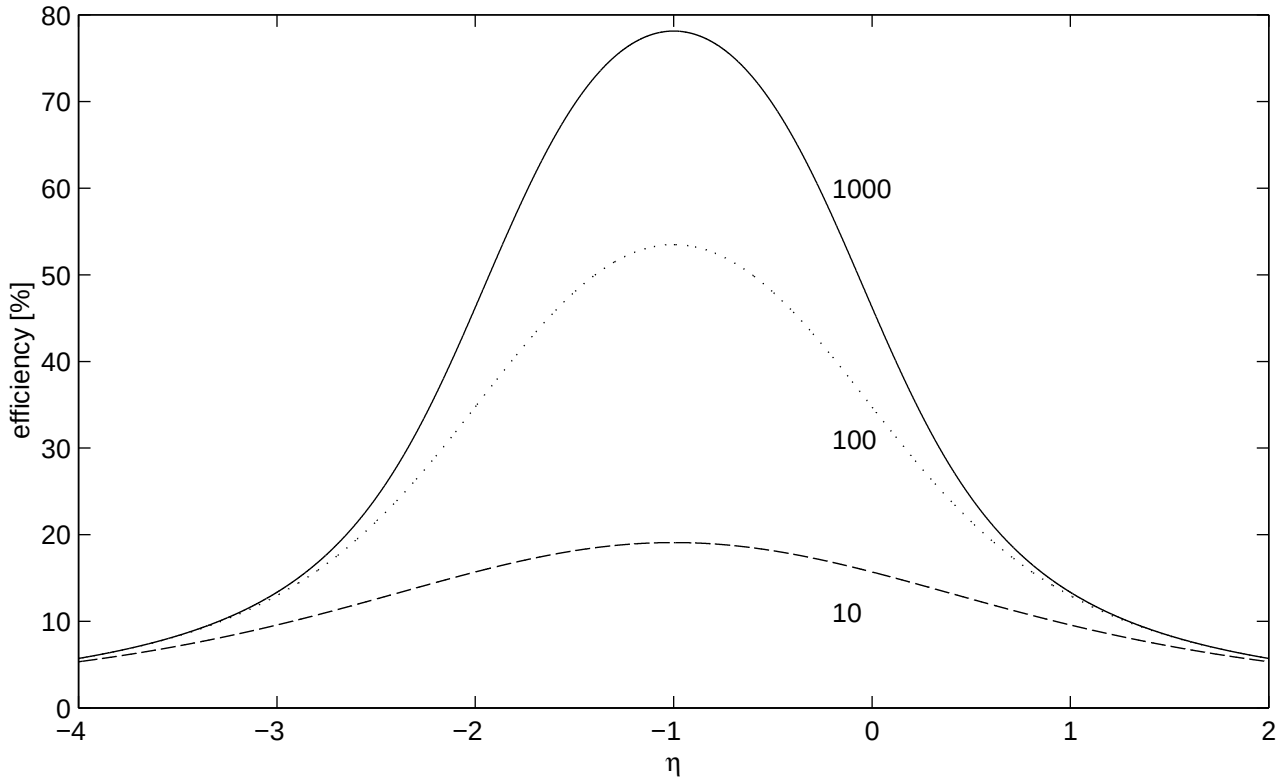
efficiency [%]
η
1000
100
10
0
10
20
30
40
50
60
70
80
−4
−3
−2
−1
0
1
2